ELSEVIER

Journal of Atmospheric and Solar-Terrestrial Physics 66 (2004) 1797–1803

Journal of ATMOSPHERIC AND SOLAR-TERRESTRIAL PHYSICS

www.elsevier.com/locate/jastp

Solar particle events seen by the MOPITT instrument

Florian Nichitiu[a,*], James R. Drummond[a], Jiansheng Zou[a], Robert Deschambault[b]

[a]*Department of Physics, University of Toronto, 60 St. George Street, Toronto, Ont., Canada, M5S 1A7*
[b]*COM DEV, Cambridge, Ont., Canada*

Received 10 November 2003; received in revised form 14 May 2004; accepted 8 June 2004

Abstract

This paper reports on Device Single Events (DSEs) occurring in the Measurements Of Pollution In The Troposphere (MOPITT) space instrument piezoelectric accelerometers. It is found that DSEs correlate with the radiation environment, solar activity and high intensity Solar Proton Events.
© 2004 Elsevier Ltd. All rights reserved.

Keywords: Solar activity; Solar proton events; Solar radio flux; Satellite anomalies; Space environment effects

1. Introduction

Since its launch on December 18, 1999 the MOPITT instrument has collected data while flying aboard the Terra spacecraft. Terra is in a sun-synchronous polar orbit, has an orbital period of 98.88 min, an altitude of 705 km, an inclination of 98.2°, and a descending node crossing time at 10:43 am.

The MOPITT instrument is an infrared gas correlation radiometer (Drummond, 1996). It operates with eight channels, four CO thermal channels at a fundamental wavelength of 4.7 μm, two CO solar channels at 2.3 μm and two CH_4 solar channels at 2.2 μm.

To maximize the signal-to-noise ratio and achieve optimal performance, the infrared detectors need to be cooled to less than 105 K. This is achieved by using a pair of 50–80 K mechanical Matra Marconi (now Astrium) Stirling Cycle Coolers.

The vibration level in each axis is measured by a triaxial piezoelectric accelerometer (Kistler Instrument AG) mounted on the compressor and displacer. Each accelerometer uses a shear mode-sensing element made of quartz. It is a multi-component force transducer, which consists of a stack of quartz discs or plates and electrodes. Each quartz disc has been cut in an appropriate axis and the orientation of the sensitive axes coincides with the axes of the force components to be measured. An internal Piezotron circuit (charge-to-voltage converter) provides a low impedance output. The units are hermetically sealed in titanium housings.

During normal operation, there are short fluctuations (spikes, lasting for only one telemetry sample), which increase the normal level of vibration by more than 4 sigma (see Fig. 1 for an example). The sensor records a normal level approximately 8 s later, the time between two consecutive telemetry samples.

These spikes, or accelerator outliers, occur much more often for the *z*-direction compressor vibrations. Outliers occur for other directions and for the displacer accelerometer, but their rate is very low (less than 5% of all the events). The occurrence of the *z*-direction

*Corresponding author. Fax: +1-416-978-8905
E-mail address: nichitiu@atmosp.physics.utoronto.ca (F. Nichitiu).

1364-6826/$ - see front matter © 2004 Elsevier Ltd. All rights reserved.
doi:10.1016/j.jastp.2004.06.002

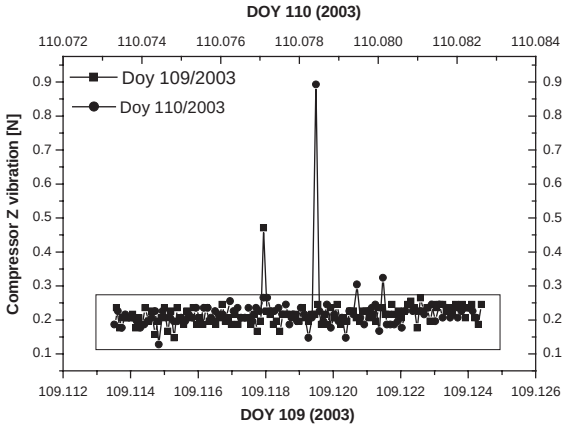

Fig. 1. Example of vibration time distribution shown by the MOPITT compressor Accelerometer: for Day of Year (DOY) = 109 and 110/2003.

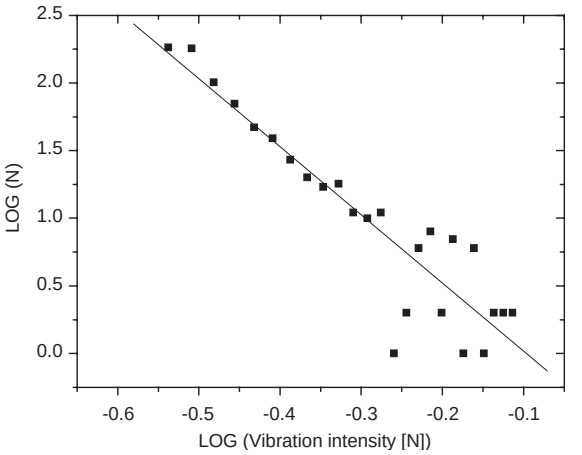

Fig. 2. Intensity distribution for all anomalous accelerometer events.

compressor transducer outliers is well described by a decreasing power-law as a function of magnitude (Fig. 2). We have investigated possible causes for this difference in sensitivity, but to date we have been unable to provide a definitive explanation.

2. Location of device single events

During the period from March 2000 to January 2003 more than 1000 accelerometer outliers were recorded, a large enough set to apply a statistically meaningful analysis. The strong localization of these events in the South Atlantic Anomaly (SAA) and Polar regions (see Fig. 3) indicate that these type of outliers are caused by the radiation environment (energetic particles) (Daly, 1994; Heynderickx, 2002). For a similar case see for example Heirtzler (2002). For a recent discussion of space radiation environment (space weather) and its effects on technological systems in space see Brautigam (2002) and Gubby and Evans (2002). Since these accelerator outliers are not specifically identified as upsets in digital circuitry—a "Single Event Upset" or SEU—we use here the term DSE for "Device Single Event" to describe them.

MOPITT DSEs occur mainly in the SAA (54%) and Polar regions (26%) as a consequence of two main sources of particles: trapped particles and those from Solar Particle Events (SPE). The fraction of background events not connected to the SSA or to Polar regions (20%) are due to the Galactic Cosmic Radiation (GCR).

2.1. The South Atlantic Anomaly

The SAA is an area of anomalously weak geomagnetic field strength caused by an offset of the

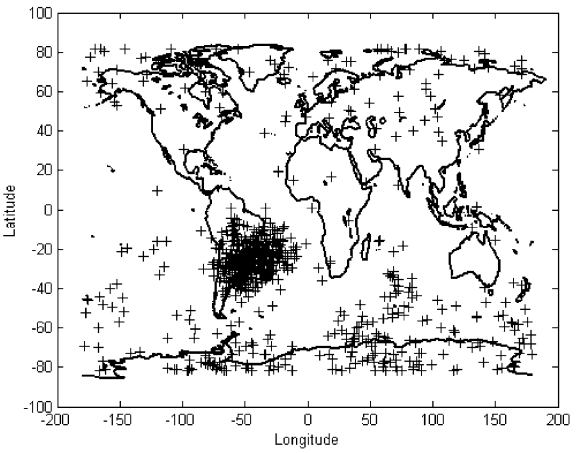

Fig. 3. MOPITT Device Single Events (DSE). Geographical distribution of DSEs. The South Atlantic Anomaly (SAA) can clearly be indentified from the point density.

geomagnetic dipole axis towards the northwest Pacific. This weak field allows radiation particles that are trapped in the Earth's magnetic field to reach lower altitudes before returning to the northern hemisphere. The daily rate of MOPITT DSEs over the SAA is 0.57 events/day (or around 9.14 events/day if it is considered that Terra is over the SAA only 6.25% of the time). The latitude and longitude distributions of DSE in the SAA region can be well fitted with a gaussian form giving the location of the SAA as: Latitude = −26.1°, Width = 16.7°, Longitude = −47.4°, Width = 28.4°.

The Day:Night ratio is 0.72:1 for events over the SAA. As the gyro radius of trapped particles can be very large, the lower rate of DSE (43.6%) on the dayside of the Earth can be understood as the effect of the neutral

atmosphere expanding during the day compared to the night and consequently the erosion of the radiation belts due to increased interaction with neutral constituents.

2.2. Polar regions and background

As can be seen in Fig. 3, there is an evident asymmetry between the North and South pole regions (North:South poles ratio 0.43:1) with more DSEs occurring in the southern hemisphere and a modest concentration of events near the south magnetic pole (66°S, 139°E). If we consider the Polar regions ($>65°$N and $>65°$S), the polar DSEs received from the MOPITT accelerometer are 25.6% of the total with almost 70% of them in the southern hemisphere.

The Day:Night asymmetry ratio for DSE received over the Polar regions is 1.04:1, which is more symmetric than for the SAA. This indicates that many of the high-energy particles causing accelerometer outliers over the Polar regions are not trapped particles, but likely come directly from the solar wind and are injected over the poles.

3. Solar proton events

Solar Proton Events (SPEs) are very large particle events with large fluxes of high-energy particles reaching the Earth (see Tranquille, 1994). SPEs are normally associated with eruptive prominences, large solar flares and Coronal Mass Ejections (CMEs) (Baker, 2000). Even though their frequency is low over a long period of time, a single SPE can have the most extreme effects on low-Earth orbit space systems as well as on the Earth's atmosphere (Jackman et al., 1999, 2001).

For the analyzed time period (993 days), the daily rate of MOPITT DSEs varies from 0.5 to 2.0 events/day and has an average value of 1.06 events/day, but during a short time interval, usually 1 or 2 days, the rate can increase by up to an order of magnitude. These high daily rates, are caused by high-intensity, high-energy SPEs as shown below.

Time series of MOPITT DSE daily rates and high-flux SPEs are shown in Fig. 4 and in Table 1 we select those events for which the daily number of DSE is at least 10 times more than the nearby average daily rate (continuous line in Fig. 4). Using the list of SPEs affecting the Earth Environment prepared by NOAA-Space Environment Center[1] we found a coincidence with 3 large SPEs for which the maximum proton flux with energies >10 MeV is larger than 10 000 pfu, 1 pfu = 1 p/(cm^2 s sr), (denoted by Y in Table 1) and two more high flux SPEs with no effect on the DSE rate (denoted N in Table 1).

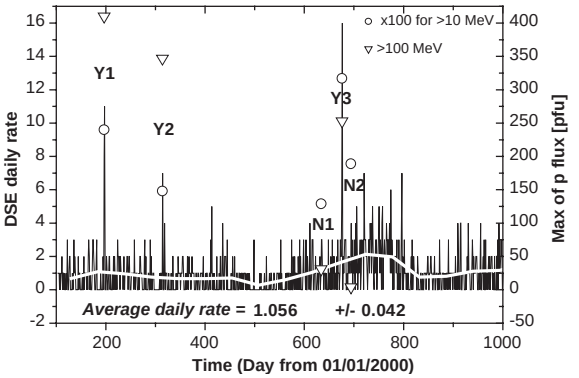

Fig. 4. Time series of DSE daily rate and correlation with SPEs. Y# (large SPEs which affect the DSE daily rate) and N# (large SPEs with no effect on the DSE daily rate) refer to SPEs identified in Table 1. The continuous white line is the daily average rate smoothed over 27 days. Note that the figures for >10 MeV fux have been scaled down by $100\times$ to fit on the plot.

In a close inspection of the high-flux SPEs it was found that the two 'quiet' SPEs are different from the other three SPEs in several respects:

The energy spectrum of these two types of SPE differ in the high-energy component. All the SPEs have comparable peak proton fluxes for particles with energy <10 MeV, but the 'quiet' SPEs have weak fluxes for particles with energies >100 MeV [2,3] (see Table 1).

Both quiet SPEs have the associated CME, flare or active region located in southern hemisphere of the solar disc while all the others are in the northern hemisphere. This is probably not relevant for our situation.

The two 'quiet' SPEs have a flatter increase of particle flux (from GOES proton flux plots [2,3]). The proton flux rises from pre-SPE level to a high value in a short time (~ 1 h) for the three significant SPEs, while for the two 'quiet SPEs' the rise time to maximum proton flux take 5–6 h.

The third solar event, the SPE of November 6, 2001, began in fact two days before it was detected by MOPITT. It began with a fast proton flux increase, followed by a second increase of proton flux after approximately 2 days which significantly increased particularly the high-energy component[2,3] (see www.sec.noaa.gov/ftpdir/plots/2001_plots/proton/20011106_proton.gif or www.sec.noaa.gov/weekly/pdf/prf1367.pdf). The high daily DSE rate was observed

[1] www.sec.noaa.gov/ftpdir/indices/SPE.txt

[2] www.sec.noaa.gov/ftpdir/plots/ : GOES Proton fluxes.

[3] www.sec.noaa.gov/weekly/

Table 1
Solar Proton Events

Event	Date	Day (from 1/1/2000)	Total DSE	DSE/Day	Max p Flux [pfu] at	
					>10 MeV	>100 MeV
Y1	Jul 14/15: 2000	196/197	19	1.03	24000	410
Y2	Nov 09: 2000	314	7	0.67	14800	347
N1	Sept 25: 2001	634	3	1.24	12900	31
Y3	Nov 06: 2001	676	16	1.59	31700	253
N2	Nov 24: 2001	694	3	1.78	18900	4

only on November 6, when the energy of particles became sufficient to register on the element of our piezoelectric accelerometer.

That the MOPITT accelerometer is sensitive to particles with high energy can be also inferred from SOHO spacecraft data. The Proton Monitor (PM) on the SOHO Spacecraft responds to ions with incident energies >50 MeV and to electrons with incident energies >2 MeV. The largest particle flares since January 1996 observed by PM on SOHO were the same 'intense' SPEs [4] (see for example http://umtof.umd.edu/pm/3flares.gif), that induce a high daily rate for MOPITT DSE.

SPEs can be characterized not only by peak flux (particles/(cm^2 s sr)), but also by the fluence which is the total number of particles greater than a specific energy experienced during an event (particles/cm^2), and SPEs with high peak fluxes are not necessarily those with high fluences. We assume that during the Solar Event, the total number of accelerometer outliers (DSEs) should be correlated with the total number of particles above the accelerometer threshold energy (event fluence for specific energy) rather with the peak flux. From the ESA Solar Proton Event Archive [5] we used the event integrated fluence fitted by an exponential in energy and calculated the SPE fluences for different threshold energies. The best correlation between total number of DSE (Table 1) and SPE fluence is shown in Fig. 5 and corresponds to a MOPITT threshold energy for the piezoelectric accelerometer of $E = 15$ MeV.

The MOPITT accelerometer outliers received during the intense SPEs (denoted by Y in Table 1) are almost all located in the polar region with an evident North/South asymmetry (see Fig. 6). A reasonable conclusion is that the high-energy particles causing accelerometer outliers during SPEs are not trapped particles, and that the Polar regions are areas of higher risk for satellites during intense SPEs.

[4] umtof.umd.edu/pm/flare/ : SOHO Proton monitor

[5] http://www.estec.esa.nl/wmwww/wma/Data_Plots/noaa/events/

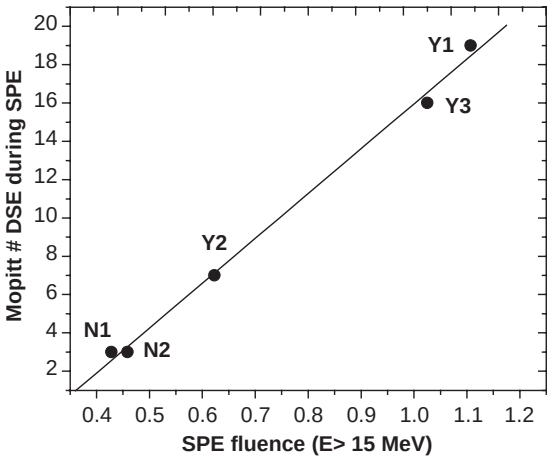

Fig. 5. Correlation between number of DSE during SPEs and the SPE proton fluence for $E>15$ MeV (in units of 10^{10} particles/cm^2). Y# and N# refer to SPEs identified in Table 1.

4. Correlations with solar activity

Many of the relevant particle sources are modulated during the course of the solar cycle. As observed from ground neutron detection, the effect of solar activity is to increase the loss of protons due to the expanding atmosphere during solar maximum and so to decrease the trapped radiation doses in LEO (Heinrich, 1994). The same anti-correlation for the integral GCR flux and solar activity is due to an increase of the Interplanetary Magnetic Field (IMF) generated by the sun (Ahluwalia, 2002).

The time distribution of the MOPITT DSE daily rate (Fig. 4) shows several increases for the time period of November 2001–February 2002 suggesting a direct connection with solar activity.

The period 2000–2003 is the maximum of Solar Cycle (SC) #23. The two main proxies used to follow the Solar Activity are Sun Spot Number provided by the S.I.D.C. Brussels International Sunspot Number (RI SSN) and

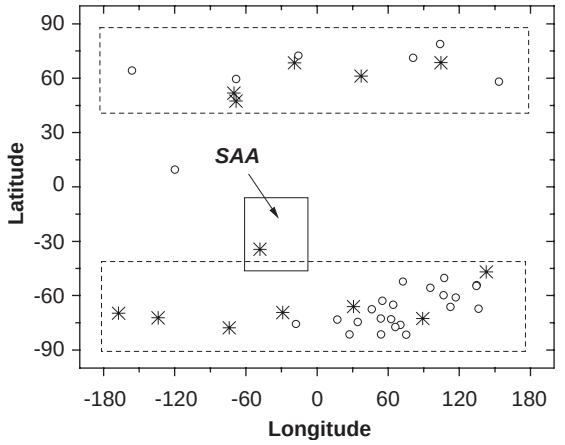

Fig. 6. MOPITT DSE location during intense Solar Proton Events (SPE). Open circles are daytime, stars are nighttime. There is only one DSE in South Atlantic Anomaly (SAA) region .

the 10.7 cm Solar Radio Flux, the F10.7 index [6, 7].The F10.7 solar radio flux is the integrated emission from the solar disc at 2800 MHz (10.7 cm wavelength) expressed in solar flux units (sfu $= 10^{-22}\,\mathrm{W\,m^{-2}Hz^{-1}}$) and is provided by Penticton Radio Observatory, B.C. Canada (Tapping, 1987). Fig. 7 shows that during this period of maximum solar activity there is in fact a general trend for both indexes to decrease from a moderate activity in the middle of 2000 to a minimum at the beginning of 2001 followed by a sharp increase in the period from November 2001 to March 2002.

The 27-day average of MOPITT DSE shows a similar trend, a minimum at the beginning of 2001 and a maximum between November 2001 to March 2002. This direct correlation with solar activity is present for events located in the SAA and the Polar regions, as well as for background events (see Fig. 8). Due to the small time scale and probably due to the higher altitude (705 km) of the spacecraft, the anti-correlation with solar activity found during the 11 year solar cycle from the ground detection is not observed.

The smoothed monthly averages of these indexes (Fig. 7) show clearly that the present SC#23 maximum is in fact a double maximum in both proxies and the well-known correlation between SSN and F10.7 index breaks down during the second solar 'sub-maximum'. A similar behavior, but much weaker, can be seen for the previous Solar Cycle: SC#22.

In Fig. 9, the 27-day smoothed average of the MOPITT DSEs received over the SAA shows a good correlation with similar averages of Solar radio flux (F10.7 index) but not with the SSN index. During the

[6]www.sec.noaa.gov/ftpdir/weekly/RecentIndices.txt
[7]ftp://ftp.ngdc.noaa.gov/STP/SOLAR_DATA/

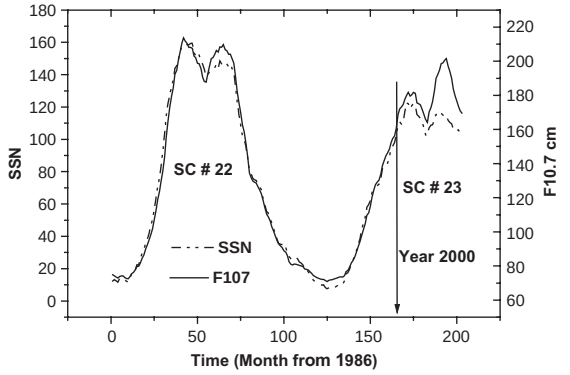

Fig. 7. Monthly smoothed Solar Spot Number (SSN)(dashed) and F10.7 (continuous) for Solar Cycle (SC)# 22 and SC#23.

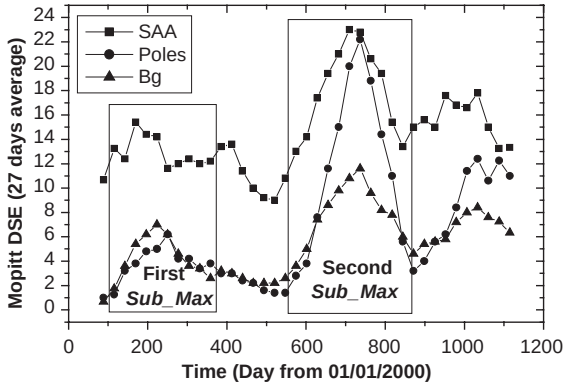

Fig. 8. 27-day average of MOPITT DSE daily rate (SAA = South Atlantic Anomaly, Bg = Background (not Poles or SAA)).

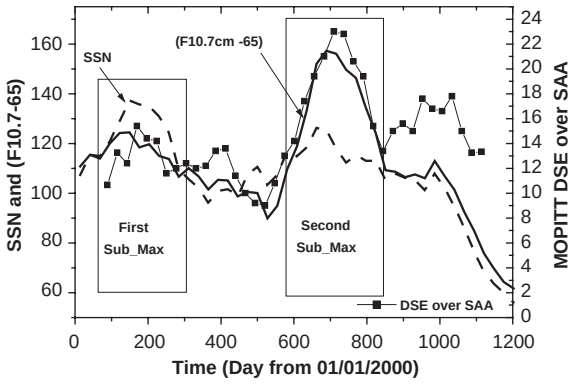

Fig. 9. Correlation of MOPITT piezoelectric accelerometer outliers with Solar activity. (a): MOPITT DSE over SAA and Solar Spot Number. (b): MOPITT DSE over SAA and 10.7 cm Solar Radio Flux.

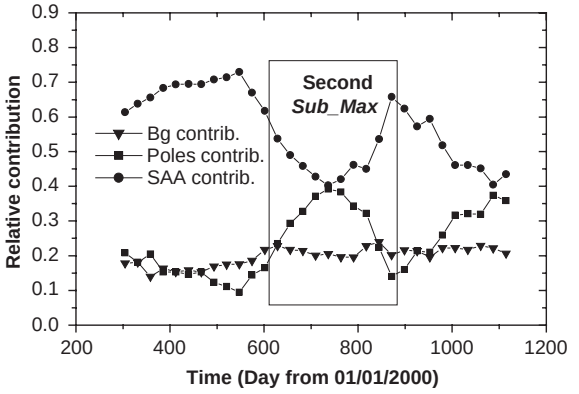

Fig. 10. The relative contribution of DSEs over South Atlantic Anomaly (SAA), Poles and Background (Bg) as a function of time.

second sub-maximum of SC#23, the number of outliers observed over the Polar regions increased dramatically whereas the background and those observed over SAA increased modestly (Fig. 8). This is interpreted as due to injection of more high-energy particles via poles relative to those over SAA, a fact that is better illustrated in Fig. 10 where the time dependence of relative contributions of SAA, Background and Polar regions to the total number of outliers is shown.

Therefore, the total number of events increases as a consequence of a general increase in solar activity (Fig. 8). The rate of DSE follows the Solar Radio flux F10.7 index not the SSN (Fig. 9), and during second Solar sub-maximum of the Solar Cycle, the fraction of high energetic particles which cause the outliers over the poles increases (Fig. 10). From these observations we can conclude that the second sub-maximum of Solar Activity maximum of SC#23 is mainly characterized by injection of more high-energy particles via the poles, a good proxy of which is the F10.7 Solar Radio flux.

5. Summary and conclusions

For more than 2 years the MOPITT piezoelectric accelerometers have recorded satellite outliers by showing short, high-intensity signals well correlated with the high-energy radiation environment.

Most of the events are recorded for the z-direction compressor vibrations which means that this specific piezoelectric layer, or its electronics, is more sensitive to high-energy particles.

Analysis of these anomalous accelerometer signals shows a direct correlation of the DSE daily rate with solar activity, a Day/Night asymmetry caused probably by interaction of trapped particles with the neutral atmosphere, and a direct correlation with high-intensity SPEs. The high-energy particles—the source of anomalous accelerometer signals—are localized mainly in SAA region, but the polar regions, particularly the southern pole, are also regions of higher risk for satellites mainly during intense SPEs.

We have also found that at least during the Solar maximum, there is a correlation of the particle population responsible for DSEs in the piezoelectric accelerometer with solar activity and this is expressed better by the F10.7 Solar Radio flux than the SSN. During the second sub-maximum of SC#23, the fraction of events over the poles relative to the SAA region increases, which means that it is probable that there are more high-energy particles of non-trapped origin in this time interval, and a good proxy for tracking this phenomenon is the F10.7 index.

Acknowledgements

The authors wish to thank Dr. J. Heirtzler, Dr. K. Tapping, and Dr. J. Kar for helpful conversations and communications. MOPITT mission and data analysis are supported by the Canadian Space Agency (CSA), Natural Sciences and Engineering Research Council (NSERC) and the National Aeronautics and Space Administration (NASA).

References

Ahluwalia, H.S., 2002. IMP intensity and galactic cosmic ray modulation. Advances in Space Research 29 (3), 439–444.

Baker, D.N., 2000. Effects of the Sun on the Earth's environment. Journal of Atmospheric and Solar-Terrestrial Physics 62, 1669–1681.

Brautigam, D.H., 2002. CRRES in review: space weather and its effects on technology. Journal of Atmospheric and Solar-Terrestrial Physics 64, 1709–1721.

Daly, E.J., 1994. The radiation belts. Radiation Physics and Chemistry 43 (1/2), 1–17.

Drummond J.R., 1996. MOPITT Mission Description Document. Department of Physics, University of Toronto.

Gubby, R., Evans, J., 2002. Space environment effects and satellite design. Journal of Atmospheric and Solar-Terrestrial Physics 64, 1723–1733.

Heinrich, W., 1994. Cosmic rays and their interactions with geomagnetic field and shielding material. Radiation Physics and Chemistry 43 (1/2), 19–34.

Heirtzler, J., 2002. The future of the South Atlantic anomaly and implications for radiation damage in space. Journal of Atmospheric and Solar-Terrestrial Physics 64, 1701–1708.

Heynderickx, D., 2002. Radiation belt modeling in the framework of space weather effects and forecasting. Journal of Atmospheric and Solar-Terrestrial Physics 64, 1687–1700.

Jackman, C.H., Fleming, E.L., Francis, M., Vitt, F.M., Considine, D.B., 1999. The influence of solar proton events

on the ozone layer. Advances in Space Research 24 (5), 625–630.

Jackman, C.H., McPeters, R.D., Labow, G.J., Fleming, E.L., Praderas, C.J., Russell, J.M., 2001. Northern Hemisphere atmospheric effects due to the July 2000 solar proton event. Geophysical Research Letters 28 (15), 2883–2886.

Tapping, K.F., 1987. Recent solar radio astronomy at centimeter wavelengths: the temporal variability of the 10.7-cm flux. Journal of Geophysical Research 92 (D1), 829–838.

Tranquille, C., 1994. Solar proton events and their effect on space systems. Radiation Physics and Chemistry 43 (1/2), 35–45.